Molecular Crystals and Liquid Crystals
Publication details, including instructions for authors and subscription information:
http://www.tandfonline.com/loi/gmcl18

Multi-Charge Carrier Trapping in Organic Crystals: Quantized Internal Macrotrap Energy Levels

J. Kalinowski [a c] & J. Godlewski [b]

[a] Istituto di Fotochimica e Radiazioni d'Alta Energia del C.N.R Bologna, 40126, Bologna, Italy

[b] Department of Molecular Physics, Technical University of Gdańsk, 80-952, Gdansk, Poland

[c] Department of Molecular Physics, Technical University of Gdansk, 80-952, Gdańsk, Poland

Version of record first published: 24 Sep 2006.

To cite this article: J. Kalinowski & J. Godlewski (1991): Multi-Charge Carrier Trapping in Organic Crystals: Quantized Internal Macrotrap Energy Levels, Molecular Crystals and Liquid Crystals, 205:1, 101-121

To link to this article: http://dx.doi.org/10.1080/00268949108032080

Mol. Cryst. Liq. Cryst., 1991, Vol. 205, pp. 101–121
Reprints available directly from the publisher
Photocopying permitted by license only

Printed in the United States of America

Multi-Charge Carrier Trapping in Organic Crystals: Quantized Internal Macrotrap Energy Levels

J. KALINOWSKI†

Istituto di Fotochimica e Radiazioni d'Alta Energia del C.N.R. Bologna, 40126 Bologna, Italy

and

J. GODLEWSKI

Department of Molecular Physics, Technical University of Gdańsk, 80-952 Gdańsk, Poland

(Received April 27, 1990; in final form April 27, 1990)

Multi-charge carrier capture by each member of a set of discrete spatially extended domains (macrotraps) is considered as a trapping mechanism responsible for the space charge evolution in the high-concentration regime of the charge introduced to organic crystals.

Finite dimension and energy depth limit the number of carriers of the same sign to be captured by such a macrotrap. Due to the Coulombic repulsion within the macrotrap, different discrete energy levels (E_k) are allowed for occupation with increasing number ($k = 1\,2, \ldots, n$) of the carriers. These energy levels can be visualized by the cascade-like pattern in the plots illustrating various electronic phenomena related to trapping and detrapping charge carriers. A detailed analysis of two such phenomena is presented: (i) the shortening of the triplet exciton lifetime by thermally-injected electrons as a function of injecting voltage in anthracene, and (ii) the fluorescence quenching by the triplet-exciton injected holes as a function of exciting light intensity in tetracene crystals. The cascade-like plots of these two dependences are interpreted in terms of the discrete energy levels characteristic of multi-charge carrier trapping by macrotraps.

Keywords: charge trapping, molecular solids, crystal defects, charge injection, photoinjection, exciton-charge carrier interactions.

1. INTRODUCTION

Many electronic processes in organic crystals are often dominated by the presence of charge traps (see e.g., References 1–4). However, the previous concepts explaining the role of traps in these processes did not take into account the essential physical factor of spatial extension of effective traps. Only recently, Kalinowski

† On leave from Department of Molecular Physics, Technical University of Gdańsk, 80-952 Gdańsk, Poland.

and coworkers[5,6] have shown that the power dependence of the current (i) versus voltage (U) under space-charge-limited (SCL) conditions can be explained by taking into account the spatial extension of charge traps in anthracene crystals. The power $n > 2$ in the relation $i \sim U^n$ has been expressed by $n = 2 + 3/\sigma$, where σ is a characteristic parameter of the exponential energy distribution function of local traps (microtraps) composing trapping extended domains (macrotraps). The spherical symmetry macrotraps of radius r_0 are characterized by the potential $E(r) = (3k_BT/\sigma)\ln(r_0/r)$[5,6] which expresses the energy (E) distribution of microtraps with the distance (r) from the deepest local state (E_t) standing for the macrotrap center, and where T is the crystal temperature and k_B is Boltzmann's constant.

The spatial extension of macrotraps leads to other important consequences for electronic processes in organic crystals as for instance to enormous increase in the trapping cross section or to trapping of more than one carrier by one trap (multicharge carrier trapping). The latter is the subject of the present paper. When two or more charge carriers are captured by one macrotrap that is when they are confined to move within a limited region of space, the dynamical state of each carrier is determined by the forces acting on the carrier and by the carrier's total energy. But if the forces are conservative, the motion is determined by the potential energy $E_p(r)$ of the carrier. This energy is composed of two parts: the interaction of the carrier with the macrotrap walls, and its interaction with other carriers captured in the macrotrap. Due to finite dimensions of the macrotrap and discrete step increment of the charge, the energy corresponding to different carrier populations in the macrotrap will form a set of discrete levels with an internal spacing decreasing with the number of captured carriers.

If an ohmic contact is used for the charge injection into a crystal with such macrotraps, the position of the quasi-Fermi-level (dependent of the stored charge and hence on the applied voltage U) scans sequentially the discrete levels, leading to a cascade pattern in various characteristics of the electronic processes determined by the injected charge. A cascade pattern behaviour has been suggested by Pope and Kallmann[7] to occur in anthracene crystals for SCLC $i-U$ dependence,[8] thermally stimulated currents (TSC),[9] and injecting voltage dependence of triplet exciton lifetime.[10–13] Such a behaviour has also been observed in tetracene crystals for the charge concentration[14,15] and light intensity dependence of the photoluminescence quenching by the injected charge.[16] This behaviour of anthracene crystals was previously interpreted by Pope and Kallmann[7] as a result of the sequential filling of discrete traps formed by dimer (or pre-dimer) clusters at crystal defect sites. They suggested that the closely spaced ($\sim k_BT$) energy levels are due to distinct jumps in the polarization energy of the trapping site with increasing number of dimer pairs in a cluster. However, a closer analysis of the experimental results leads to contradictions between the data obtained from such an interpretation and those based on independent measurements. For instance, the value of the cross section $A = \nu/\upsilon N_{\text{eff}} = 2.5 \times 10^{-15}$ cm^2 for electron capture by a typical point defect (with the frequency factor $\nu = 10^{12}$ s^{-1}, $N_{\text{eff}} = 4 \times 10^{21}$ cm^{-3} and $\upsilon = 10^5$ cm/s)[17] is about four orders of magnitude smaller than $A = (N_t\upsilon\tau_c)^{-1} = 2 \times 10^{-11}$ cm^2 obtained with the density of traps $N_t = 5.4 \times 10^{12}$ cm^{-3} calculated from the trap-filled-limit voltage ($V_{\text{TFL}} = 750$ V in Figure 2 of Reference 7) and trapping

time $\tau_c = 10^{-7}$ s as measured independently with the same crystal.[10] This enormous discrepancy can be resolved if the traps are treated as macrotraps of average dimension $2\,r_0 \simeq 500$ Å and effective density of states $N_{\text{eff}} = 5 \times 10^{17}\ \text{cm}^{-3}$ as a quantity disconnected from direct relation to the molecular density. These values of r_0 and N_{eff} fall in the range of the corresponding quantities determined from the experimental SCLC $i-U$ characteristics for anthracene crystals, interpreted in terms of the macrotrap model.[5,6] Thus, the cascade pattern of the above mentioned processes can be explained either by the multi-charge trapping in one type discrete macrotraps or trapping by a set of discrete macrotraps distributed somehow in energy.

If one naturally assumes the latter distribution to follow a decreasing function of macrotrap concentration with macrotrap depth, then the voltage step in the jumps of triplet exciton lifetime should increase with the voltage applied to the crystal. This is a simple consequence of the proportionality of the injected charge to this voltage and the increasing concentration of shallower traps. However, there is no such a simple regularity as show the experimental data of Levinson *et al.*,[10] Weisz *et al.*[11] and Ern *et al.*[12] adapted and presented by Pope and Kallmann in their Figures 2 and 3.[7]

This suggests that the cascade pattern of various characteristics of the electronic processes in anthracene-like crystals can be determined by a set of discrete levels occurring as a result of multi-charge trapping in quasi-single-energy discrete macrotraps. In this paper we present a calculation of these energy levels and discuss the results in the light of existing experimental data.

2. ENERGY LEVELS IN CHARGED MACROTRAP

A. Approximation of Continuous Charge Distribution

We use the model of the macrotrap consisting of a large number of microtraps distributed in energy (E) according to the exponential function

$$h_0(E) = \frac{H_0\sigma}{k_B T} \exp(-\sigma E/k_B T), \tag{1}$$

where H_0 is the concentration of microtraps. The microtraps are homogeneously distributed in space within each macrotrap but their energy is a function of their coordinates. This function forms the macrotrap potential in the absence of charge and electric field, and in the spherical symmetry approximation can be expressed as[5]

$$E_0(r) = \begin{cases} \dfrac{3k_B T}{\sigma_1} \ln \dfrac{r_{01}}{r} & \text{for} \quad r_{01} \geqslant r \geqslant r' \\ \dfrac{3k_B T}{\sigma_2} \ln \dfrac{r_{02}}{r} & \text{for} \quad r' \geqslant r \geqslant r_b, \end{cases} \tag{2}$$

where r' is a distance from the center of the macrotrap for which $(3k_BT/\sigma_1)\ln(r_{01}/r') = (3k_BT/\sigma_2)\ln(r_{02}/r')$ and r_b stands for the dimension of the basal pinning trap.

In Equation (2) $r_{01} = r_0$ is the radius of the macrotrap given by[5]

$$r_0 = \left(\frac{3H_0}{4\pi N_0 N_m}\right)^{1/3} \tag{3}$$

with N_0 defining the concentration of macrotraps and N_m—the molecular density.

Consider, for simplicity, a one-component attractive potential

$$E_0(r) = \frac{3k_BT}{\sigma}\ln\frac{r}{r_0} \tag{4}$$

fulfilling the following conditions:

$$\begin{aligned} E_0 &= 0 \qquad \text{for} \quad r = r_0 \\ E_0 &= -E_{0t} \quad \text{for} \quad r = r_b, \end{aligned} \tag{5}$$

and

$$\left(\frac{dE}{dr}\right)\cdot a \ll kT. \tag{6}$$

The introduction of $N > 1$ one-sign elementary charges (e) into a macrotrap will modify potential (4) by an additional term E_q resulting from the Coulombic repulsion of the N charge carriers‡

$$E(r) = \frac{3k_BT}{\sigma}\ln\frac{r}{r_0} + E_q(r). \tag{7}$$

In order to obtain E_q in an analytical form let us separate one of the carriers and locate it at site P (see Figure 1). The remaining carriers will be considered as continuously distributed charge in the macrotrap on a spherical surface of radius r with the density

$$\eta = \frac{Ne}{4\pi r^2}. \tag{8}$$

For the carrier $q = e$ at site P, the interaction energy with a strip of the surface charge $dq' = 2\pi r_\theta r\eta d\theta$ is

$$dE_q = \frac{q\,dq'}{4\pi\varepsilon\varepsilon_0\xi} = \frac{q\eta r_\theta r d\theta}{2\varepsilon\varepsilon_0\xi}, \tag{9}$$

‡ We neglected a possible modification of the trap potential (2) by the introduction only one carrier in it.

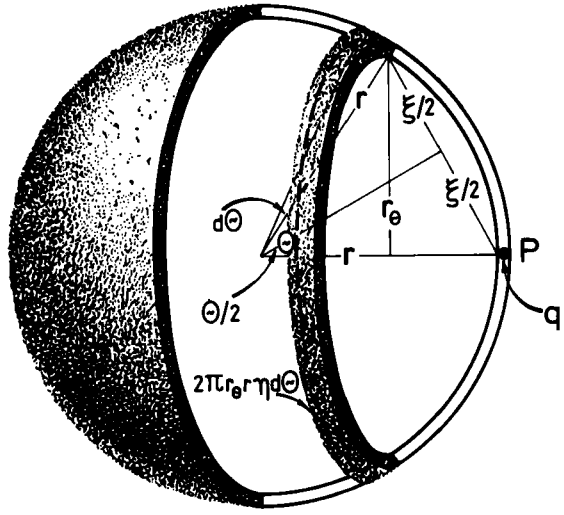

FIGURE 1 Continuous charge distribution approximation in the calculation of potential energy of Ne carriers located on a spherical surface with radius r.

where ε is the dielectric constant of the medium and ε_0 is the permittivity of free space. For the meaning of other symbols see Figure 1.

Expressing r_θ and ξ by r we readily find

$$dE_q = \frac{e^2 N \cos(\theta/2)}{8\pi\varepsilon\varepsilon_0 r} d\theta. \tag{10}$$

Integrating Equation (10) yields:

$$E_q = \frac{e^2 N}{8\pi\varepsilon\varepsilon_0 r} \int_{\phi N}^{\pi} \cos(\theta/2) d\theta = \frac{e^2 N}{4\pi\varepsilon\varepsilon_0 r} \left(1 - \sin\frac{\phi_N}{2}\right). \tag{11}$$

The lower limit of integration is not equal zero because we separated one elementary charge for which the angle ϕ_N must be set apart according to

$$\int_0^{\phi N} 2\pi r^2 \sin\theta \, d\theta = \frac{4\pi r^2}{N} \tag{12}$$

and, thus

$$\phi_N = \arccos\left(1 - \frac{2}{N}\right). \tag{13}$$

Insertion of $E_q(r)$ from Equation (11) into Equation (7) results in the effective potential energy function

$$E(r) = \frac{3k_BT}{\sigma} \ln \frac{r}{r_0} + \frac{e^2N}{4\pi\varepsilon\varepsilon_0 r} \left(1 - \sin \frac{\phi_N}{2}\right). \tag{14}$$

It has a minimum at a position r_m, where

$$r_m = \frac{e^2N\sigma \left(1 - \sin \frac{\phi_N}{2}\right)}{24\pi\varepsilon\varepsilon_0 k_BT} \tag{15}$$

and at the minimum the potential is given by

$$E_m = \frac{3k_BT}{\sigma} \left(2 + \ln \frac{r_m}{r_0}\right) \tag{16}$$

as it is shown in Figure 2.

We notice that $|E_m| \leqslant |E_t|$, so that even for $N = 1$, $r_m = 0$ and is limited by $r = r_b$.

The trapping energy E_t (the depth of trap) can thus be expressed as

$$E_t = \delta E - E_m = \frac{e^2N[1 - \sin(\phi_N/2)]}{4\pi\varepsilon\varepsilon_0 r_0} - \frac{3k_BT}{\sigma} \left(2 + \ln \frac{r_m}{r_0}\right), \tag{17}$$

where δE is defined on Figure 2 showing energy diagrams deduced from Equation (14).

An inspection of Equation (17) allows us to conclude that the attractive potential appears only within a certain range of N; the range being dependent on the parameters σ and r_0.

A few examples of $E_t(N)$ for different σ and r_0 are shown in Figure 3. The trapping will take place only if the energy $E_t > 0$. In Figure 3 it is seen that for a certain number (dependent on r_0 and σ) of the carriers captured by the macrotrap $E_t = 0$ and then even $E_t < 0$. The smaller is σ the larger is the number N for which $E_t \leqslant 0$ (the trap becomes a scattering center). For typical macrotraps (250 Å $\leqslant r_0 \leqslant$ 1000 Å and $0.3 \leqslant \sigma \leqslant 1.0$) the limiting values of N_{lim} for which $E_t = 0$ are contained within the range $4 \leqslant N_{\text{lim}} \leqslant 30$. However, for highly extended domains ($r_0 \sim 1$ μm) and $\sigma \sim 0.3$, N_{lim} can be larger than 30. We notice that the positive values of E_t for large $N > N_{\text{lim}}$ do not have any real meaning because $r_m > r_0$ in this range of N (cf. Figure 4).

B. Discretization of Energy

Since the charge Q captured by one macrotrap can be changed discretely

$$Q = \sum_N q_N \quad (N = 1, 2, 3, \ldots, n), \tag{18}$$

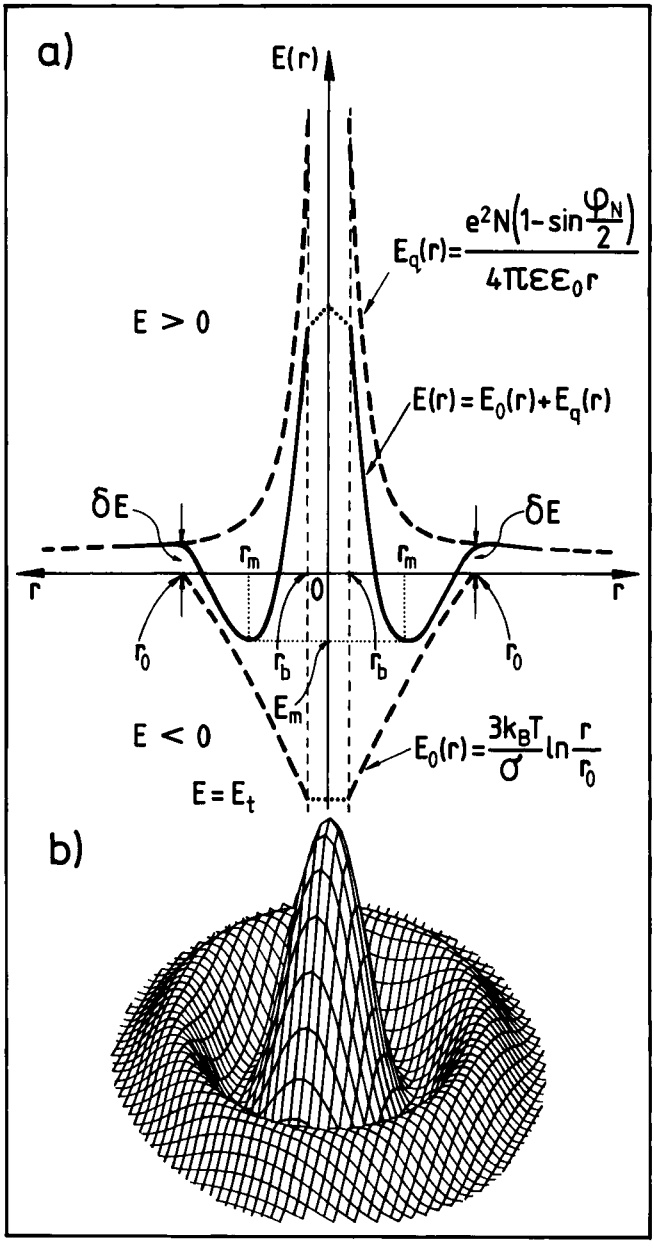

FIGURE 2 Schematic potential energy diagrams according to Equation (13) in one-(a) and three (b)-dimensional representation. The macrotrap $E_0(r)$ and Coulombic $E_q(r)$ energies are shown in part (a).

ϕ_N takes discrete values [see Equation (13)] and the Coulombic repulsion energy must be discretized as results from Equation (11) obtained from a continuous approximation of the charge distribution in a macrotrap.

On the other hand, the Coulombic repulsion energy can be expressed by

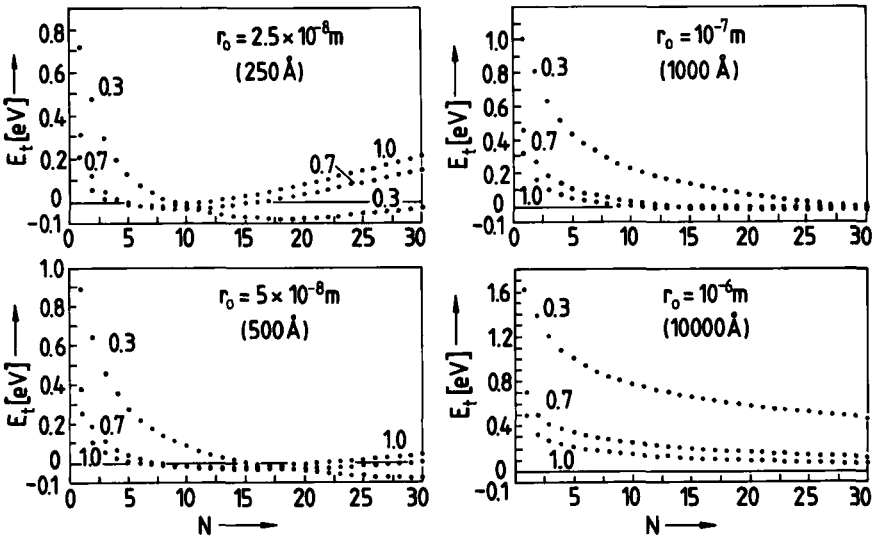

FIGURE 3 Trapping energy of a carrier (e) as a function of number (N) of charges captured by macrotraps with different radii (r_0) [Equation (13)]. The numbers standing by the curves are values of the parameter σ. The calculations have been made with $\varepsilon = 3.2$ and $r_b = 15$ Å.

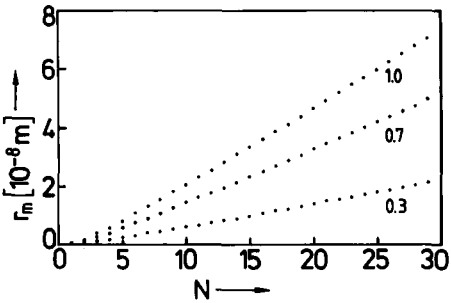

FIGURE 4 The potential minimum position (r_m) as a function of number (N) of charge carriers (e) within the macrotrap. The data calculated according to Equation (15); the numbers standing by the plots are values of the parameter σ.

$$E_N(r) = \frac{e^2}{4\pi\varepsilon\varepsilon_0}\frac{C_N}{r}, \tag{19}$$

where C_N is a number factor dependent on N.

C_N and thus $E_N(r)$ can easily be calculated in all cases of simple symmetry. A few examples of such calculations are displayed in Table I, where the values of E_N are compared with those determined from the continuous approximation formula for E_q (11). As we can see the largest error in the calculation of the repulsion energy resulting from replacing E_N by its continuous approximation E_q does not exceed 20% and for $N > 3$ is smaller than 10%. Keeping this in mind we calculated the energy levels according to Equation (17) and their sequence for different r_0 and σ is shown in Figure 5.

TABLE I

N	C_N	E_N [1]	ϕ_N [2]	E_q [1]	E_q/E_N	Relative difference [%]
2	$1/\sqrt{3}$	0.500	1.570	0.586	1.172	17.2
3	$2/\sqrt{3}$	1.154	1.230	1.270	1.101	10.1
4	$3\sqrt{6}/4$	1.840	1.047	2.000	1.086	8.6
6	$5/\sqrt{2}$	3.530	0.840	3.550	1.046	4.6

[1] The energy expressed in units $(e^2/4\pi\varepsilon\varepsilon_0 r)$.
[2] The angle expressed in radians.

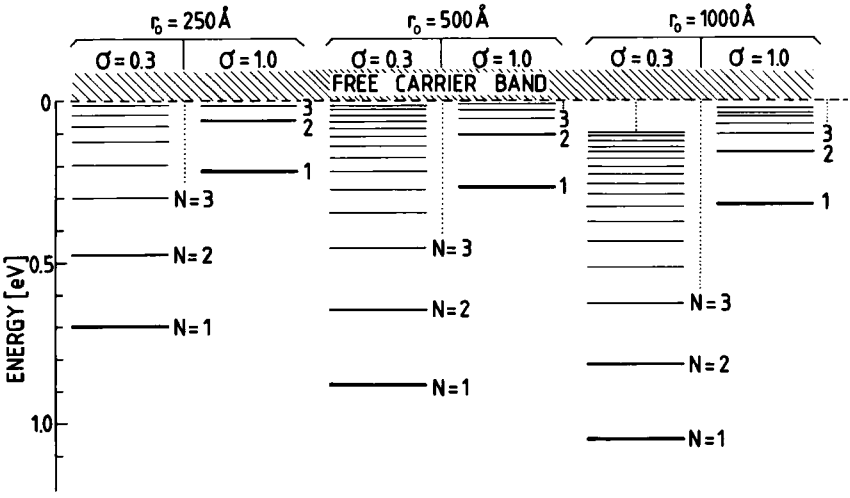

FIGURE 5 Discrete energy levels of an elementary charge carrier (e) in macrotraps with different radii (r_0) and parameters σ. Calculated according to Equation (17) with other numerical parameters as in Figure 3.

Successive energy levels, corresponding to N and $N' = N + 1$, are separated by the amount ΔE_t decreasing with increasing N for any r_0 and σ. The amount ΔE_t (1–2) $= E_t(N = 1) - E_t(N = 2)$ is the largest. For a given r_0 it decreases with σ. It is worthy to note that ΔE_t (1–2) is only slightly dependent on r_0 but is a relatively strong function of r_b. The parameter r_b determines the position E_t (1); increasing r_b leads to decreasing the one-carrier trap depth, that is E_t for $N = 1$. When the difference between two trapping levels belonging to two adjacent levels with $N \gg 2$ is taken into consideration, the $\Delta E_t < kT$ results from Equation (17) (cf. Figure 5).

The utility of the latter case cannot often be tested because it requires the crystals with low concentration of large and deep macrotraps, the condition difficult to fulfill due to relatively high probability of creation of shallower macrotraps in their growing and handling processes.

If we let macrotraps be distributed in r_0, r_b and σ, then the trapping levels

originating from different multi-charge occupation numbers (N) will overlap leading to a non-regular sequence in separation between the trapping levels.

3. COMPARISON WITH EXPERIMENT

A. Voltage Dependence of the Triplet Lifetime

Interaction of triplet excitons with charge carriers injected into a crystal creates an additional channel for radiationless decay of the excitons and makes their decay constant (β) larger as compared with its value β_0 in the absence of charge in the crystal. From the steady-state diffusion equation for excitons it follows that[1,4,10-14]

$$\beta \simeq \beta_0 + K_{Tt}\langle n_t \rangle, \tag{20}$$

where K_{Tt} is the triplet-trapped charge carrier interaction rate constant and $\langle n_t \rangle$ is the average concentration of trapped charge carriers in the interaction region.§

With an ohmic injecting electrode and interelectrode distance d[19]

$$\langle n_t \rangle \simeq \frac{3}{2}\frac{\varepsilon\varepsilon_0 U}{ed^2}, \tag{21}$$

so that β is proportional to the injecting voltage U.

The cascade-like pattern of $\beta(U)$ measured by several workers in anthracene crystals[10-13] suggests, therefore, sequential filling of discrete traps by injected charge carriers.[7] An example is shown in Figure 6. Trap-filled segments correspond to consecutive trapping levels which are defined by the position of quasi-Fermi level E_F as (see e.g., Reference 19)

$$E_t = E_F = k_B T \ln \frac{N_{\text{eff}}}{\theta n_{t\text{TFL}}}. \tag{22}$$

Combining Equations (22) and (20) connects directly the trapping levels with measured $\Delta\beta_{\text{TFL}} = \beta_{\text{TFL}} - \beta_0$:

$$E_t = k_B T \ln \frac{N_{\text{eff}} K_{Tt}}{\theta \Delta\beta_{\text{TFL}}}. \tag{23}$$

For two adjacent (i, k) levels

$$\Delta E_{tik} = E_t(i) - E_t(k) = k_B T \ln \frac{\theta_k \Delta\beta_{\text{TFL}}(k)}{\theta_i \Delta\beta_{\text{TFL}}(i)}. \tag{24}$$

§ Here we have made two following assumptions: (i) the triplet exciton-free charge carrier interaction term $K_{Tf} n_f \ll K_{Tt} n_t$ [which is reasonable in all the cases with $n_f/n_t \simeq \theta < 10^{-2}$ (see References 1, 4)] and (ii) the redistribution of triplet exciton concentration due to reabsorption and light-guide effects can be neglected (cf. Reference 18).

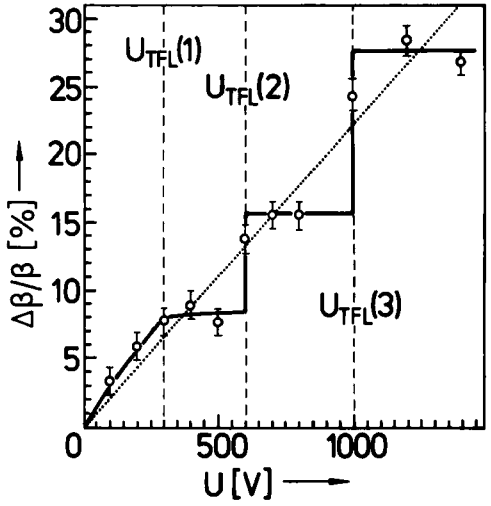

FIGURE 6 Relative increase in triplet exciton monomolecular decay rate constant as a function of injecting voltage in an anthracene crystal. Crystal thickness 210 μm, $\beta_0 = 310\ s^{-1}$. Electron injecting contact. Dotted line indicates the averaged dependence of $\Delta\beta/\beta_0$ as resulted from the standard interpretation assuming a continuous increase in the charge density proportional to the injecting voltage; solid line indicates sequential filling of macrotraps with consecutive charge carriers; vertical dashed lines separating different trap-filled segments according to interpretation of present paper. Figure adapted from Levinson *et al.*[10]

In the standard approach with infinitely sharp wall (ISW) point traps (see References 5 and 6) it can be assumed that $\theta_i \simeq \theta_k$ and

$$\Delta E_{tik} = E_t(i) - E_t(k) = k_B T \ln \frac{\Delta\beta_{\mathrm{TFL}}(k)}{\Delta\beta_{\mathrm{TFL}}(i)}. \tag{25}$$

The energy separation between level 1 and 2, calculated according to Equation (25) with suitable $\Delta\beta_{\mathrm{TFL}}$ taken from Figure 6, equals $\Delta E_{t12} = 0.017\ \mathrm{eV} < k_B T$ at room temperature. This interlevel spacing is much smaller than even the smallest separation between multi-charge trapping levels 1 and 2 for $\sigma = 1.0$ (see Figure 5). At first glance, this result might seem to clash with the interpretation in terms of multi-charge trapping concept.

However, there is no conflict because in the macrotrap model θ is a function of injecting voltage[5,6] and formula (25) cannot be used for evaluation of ΔE_{tik}. Instead, expression (24) should be applied with $\theta_i \neq \theta_k$.

For the first two levels (1, 2) the voltage dependence of θ with $E_t = E_t$ ($N = 1$) can be used as derived previously by Kalinowski *et al.*[5,6]:

$$\theta \simeq \frac{N_{\mathrm{eff}}}{N_0} \left(\frac{2.7 e r_0 \sigma}{3 k_B T}\right)^{3/\sigma} \left(\frac{U}{d}\right)^{3/\sigma} \exp(-E_t/k_B T). \tag{26}$$

Then

$$\theta_2/\theta_1 = (U_2/U_1)^{3/\sigma}, \tag{27}$$

where U_2 and U_1 are the voltages at the beginning and the end of the first TFL (flat) segment, respectively. If we put $U_2 - U_1 = \Delta U_{12}$ and substitute Equation (27) in Equation (24), the interlevel spacing can be expressed as follows:

$$\Delta E_{t12} = k_B T \ln \left[\left(1 + \frac{\Delta U_{12}}{U_1} \right)^{3/\sigma} \frac{\Delta \beta_{\mathrm{TFL}}(2)}{\Delta \beta_{\mathrm{TFL}}(1)} \right]. \tag{28}$$

It is thus apparent that both height $[\Delta\beta_{\mathrm{TFL}}(2)/\Delta\beta_{\mathrm{TFL}}(1)]$ and length (ΔU_{12}) of the steps in the cascade pattern of the voltage dependence of β are measure of the energy interlevel spacing. To obtain an idea of the values of ΔE_{t12} we assume typical $\sigma = 0.3$ (see References 5 and 6) and use the experimental results of Figure 6, $U_1 = 300\mathrm{V}$, $\Delta U_{12} = 300\mathrm{V}$, and $\Delta\beta_{\mathrm{TFL}}(2) = 0.16\ \beta_0$ and $\Delta\beta_{\mathrm{TFL}}(1) = 0.08\ \beta_0$. Then $\Delta E_{t12} = 0.2$ eV follows according to Equation (28). This value is close to $\Delta E_t\,(1\text{–}2) = 0.22$ eV—the energy separation between the one- and two-carrier occupied macrotraps with $r_0 = 250$ Å, $r_b = 15$ Å and $\sigma = 0.3$ (see Figure 5). The one-carrier occupied trap depth $E_t(1) = 0.7$ eV is the value often deduced from thermally-stimulated-current (TSC) measurements for anthracene crystals.[9,20–23] $\Delta E_{t23} = 0.14$ eV calculated in a similar way from Figure 6 with $U_2 = 600\mathrm{V}$, $\Delta U_{12} = 400\mathrm{V}$, $\Delta\beta_{\mathrm{TFL}}(3) = 0.275\ \beta_0$ and $\Delta\beta_{\mathrm{TFL}}(2) = 0.16\ \beta_0$, and $\sigma = 0.3$ is comparable with $\Delta E_t\,(2\text{–}3) = 0.16$ eV equal to the energy separation between two- and three-carrier occupied macrotraps as shown in Figure 5 for $r_0 = 250$ Å and $\sigma = 0.3$. However, in the latter case we have to be aware of an approximation made by using Equation (26) which has been derived for one-carrier occupied trap,[5,6] so that an additional lowering of the barrier due to inter-carrier repulsion is neglected. A detailed study of this case will be the subject of our further work.

B. Light Intensity Dependence of the Photoluminescence Quenching by the Charge

Figure 7 shows the experimental results on photoluminescence quenching by the charge injected to a tetracene crystal from the illuminated water electrodes, independent of their electrical bias.[15] Apparent is the cascade-like pattern in the plot of the quenching efficiency as a function of light intensity. When a tetracene crystal is illuminated in the singlet absorption region, nearly all the absorbed photons produce pairs of triplet excitons because the fission of a singlet exciton into two triplet excitons is the dominant decay channel at room temperature and ambient pressure.[24–30] The triplet excitons formed from the fission process recombine (exciton fusion) to form singlets when the excitation intensity is sufficiently high. When the exciton fusion process is operative, there is therefore an increase in the overall quantum efficiency of fluorescence.[1,4,16,27–29] The total fluorescence intensity (F_{TOT}) is then composed of two parts: prompt (F_P) and delayed (F_{DF}) fluorescence intensity,

$$F_{\mathrm{TOT}} = F = F_P + F_{\mathrm{DF}} = \frac{k_F}{k_{\mathrm{TOT}}} (\alpha I + \gamma_{TS}[T]^2), \tag{29}$$

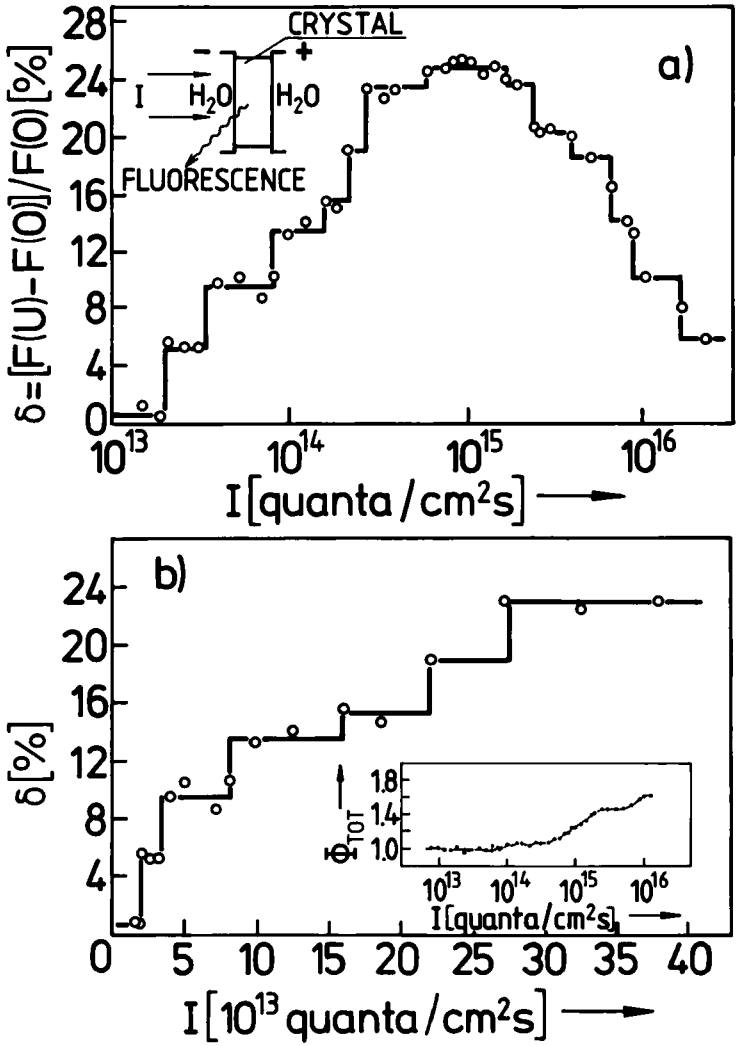

FIGURE 7 Relative increase in the total fluorescence intensity at λ_F = 560 nm of a tetracene crystal, imposed by a negative voltage U = 25 V applied to the illuminated water/tetracene crystal intersurface as a function of exciting light intensity. Crystal thickness 10 μm, wavelength of the exciting light λ_{ex} = 436 nm. The results are presented for the broad-range of the exciting light intensity in a semi-logarithmic scale (a) and for the increasing part of the dependence in a linear coordinate system (b). The light intensity dependence of the relative luminescence efficiency Φ_{TOT} shown in the inset of part (b). Figure adapted from Kalinowski and Godlewski.[16]

where k_F and k_{TOT} are the first order rate constants of the radiative and all channels singlet exciton decay, respectively; α is the absorption coefficient of the exciting light of local intensity I; $[T]$ is the concentration of triplet excitons and γ_{TS} is the second order rate constant for their fusion into a singlet exciton. In the absence of the voltage applied to the crystal and with a high exciting light flux a large concentration of charge is introduced by triplet exciton injection into the crystal region near the illuminated water contact.[31,32] The triplet exciton quenching by

injected charge becomes an additional path for triplet exciton decay diminishing the triplet exciton concentration and decreasing the DF intensity F_{DF}. A negative voltage applied to the illuminated surface (see Figure 7) removes the injected holes from the emission region and F_{DF} increases; the difference can be observed as a relative increase in the total luminescence intensity (29):

$$\delta = \frac{F(U) - F(0)}{F(0)} = \frac{[T(U)]^2 - [T(0)]^2}{(\alpha I/\gamma_{TS}) + [T(0)]^2}. \tag{30}$$

The average values of suitable triplet exciton $\{[T(U)], [T(0)]\}$ and charge carrier $[n_{tot}(U), n_{tot}(0)]$ concentrations within the penetration depth (α^{-1}) of the exciting light can be used for a rough description of the quenching. Then, neglecting exciton diffusion and the singlet exciton-charge carrier interaction, one can distinguish two cases with the following solutions:

Case I: Low light intensity ($I < 5 \times 10^{14}$ quanta/cm^{2}s) with

$$\beta[T] >> \gamma_{TOT}[T]^2 \quad \text{and} \quad \alpha I >> \frac{1}{2}\gamma_{TS}[T]^2, \tag{31}$$

and

$$[T] \simeq \frac{k_s}{k_{TOT}} \frac{\alpha}{\beta} I, \tag{32}$$

where β is the overall first order rate constant for triplet exciton decay and γ_{TOT} is the second order rate constant for triplet-triplet exciton annihilation $\{\gamma_{TS} = (1/2)f\gamma_{TOT}, f = 0.66 \pm 0.06$ (Reference 29)$\}$. According to Equations (30) and (32) an Equation for the quenching of the luminescence can now be derived as

$$\delta \simeq \alpha\gamma_{TS}\left(\frac{k_s}{k_{TOT}}\right)^2 \{[\beta(0)]^{-2} - [\beta(U)]^{-2}\}I. \tag{33}$$

Case II: High light intensity ($I > 10^{16}$ quanta/cm^{2}s) with

$$\beta[T] << \gamma_{TOT}[T]^2 \quad \text{but still} \quad \alpha I >> \frac{1}{2}\gamma_{TS}[T]^2, \tag{34}$$

and

$$[T] = \left(\frac{k_s \alpha I}{k_{TOT}\gamma_{TOT}}\right)^{1/2}. \tag{35}$$

Because any of the quantities composing Equation (35) does not depend on U, $[T(0)] = [T(U)]$ and $\delta = 0$. Indeed, for $I_0 > 10^{16}$ quanta/cm^{2}s, $\delta \to 0$ leaving for

understanding the δ behaviour in the intermediate region of intensities $5 \times 10^{14} \lessapprox I \lessapprox 10^{16}$ quanta/cm^{2}s.

The light intensity dependence of δ can be described on the basis of an analysis of the first order rate constant

$$\beta = \beta_0 + K_{\mathrm{Th}} n_t + R_{\mathrm{Th}} n_f \tag{36}$$

which is determined by the spontaneous (natural) triplet exciton decay ($\beta_0 = 2 \times 10^4$ s^{-1})‖ and the triplet exciton quenching by trapped (n_t) and free (n_f) charge carriers with respective interaction constants K_{Th} and R_{Th}.

The charge concentrations are governed by the following steady-state Equations:

$$\frac{dn_f}{dt} = A[T] + B[T]n_t - k_t n_f - k_r n_f = 0, \tag{37}$$

$$\frac{dn_t}{dt} = k_t n_f - B[T]n_t = 0. \tag{38}$$

From Equations (37) and (38) follows that

$$n_t = \frac{A}{B}\frac{k_t}{k_r} \tag{39}$$

is independent of light intensity, and

$$n_f = \frac{A}{k_r}[T] \tag{40}$$

is proportional to the triplet exciton concentration.

Here A is the rate constant for excitonic injection of charge from the aqueous contact, B is the second order rate constant for the triplet exciton-trapped carrier interaction leading to the release of the carrier from a trap, k_t is the trapping rate constant, and k_r is the recombination constant of a carrier at the crystal/water interface.

These two results are natural consequence of the fact that the triplet excitons created by exciting light are both the agents generating and detrapping the carriers. We suppose that in the low-light intensity (LLI) case

$$\beta = \beta_t \simeq \beta_0 + K_{\mathrm{Th}} n_t, \tag{41}$$

i.e. we consider only the interaction of mobile triplet excitons with trapped charge carriers.

‖ The lifetime of triplet excitons in crystalline tetracene is not precisely known, the scatter over an order of magnitude to be found in the literature. The values $\beta_0 > 10^5$ s^{-1} (see e.g., References 33, 34) are ascribed to the lifetime of a triplet trap[34] and therefore an average value of β_0 below 10^5 s^{-1} is taken for the present discussion.

Under conditions in which $n_t(I) \simeq$ const (cf. Equation (39)) the quenching efficiency is an increasing function of the exciting light intensity as follows from Equation (33) and confirmed by the general tendency in the experiment (see Figure 7).

In the intermediate range of I the third term in Equation (36) cannot be neglected and we have to take into account Equation (40). Combining in some approximations Equations (30), (32), (36) and (40) yields

$$\delta \simeq \frac{\gamma_{TS} k_r^2}{2A^2 R_{Th}^2 \alpha I} \{[\beta_t(0)]^2 - [\beta_t(U)]^2\}, \tag{42}$$

which, in contrast to Equation (33), makes the quenching efficiency a decreasing function of I. This behaviour of Equation (42) agrees with the experimental observation presented in Figure 7a.

Let us now consider the light intensity dependence of the quasi-Fermi level with $U = 0$ for the above two approximations of β.

Approximation I: $\beta \simeq \beta_t$, $I \ll 5 \times 10^{14}$ quanta/cm^{2}s.
Trap-filled segments of δ (see Figure 7b) correspond to consecutive trapping levels which coincides with the position of quasi-Fermi level similar to that in Equation (22):

$$E_t = E_F \simeq k_B T \ln \frac{N_{eff}}{\theta n_{tTFL}} = k_B T \ln \frac{G}{I[1 - \beta(U)/\beta(0)]}, \tag{43}$$

where G is a constant dependent on the concentration and energy distribution of macrotraps, the effective density of states, absorption coefficient of the exciting light and parameters characterizing the processes of trapping and detrapping charge carriers as well as the process of charge injection and properties of excitons themselves. In deriving Equation (43) we used expression (32). The energy spacing between two adjacent (i, $k = i + 1$) trapping levels is thus given by

$$\Delta E_{tik} = k_B T \ln \frac{I_k}{I_i} \frac{\{1 - [\beta_1(U)/\beta_1(0)]\}}{\{1 - [\beta_k(U)/\beta_k(0)]\}}. \tag{44}$$

With $\beta_i(U) = \beta_k(U) = \beta_0$, using Equation (33) we find

$$\Delta E_{tik} = k_B T \ln \frac{I_k}{I_1} \frac{\{1 - [1 - (\beta_0^2 \delta_k / \alpha \gamma_{TS} I_k)]^{1/2}\}}{\{1 - [1 - (\beta_0^2 \delta_i / \alpha \gamma_{TS} I_i)]^{1/2}\}} \tag{45}$$

which relates directly ΔE_{tik} with the light intensity dependence of δ.

The limiting values of I, δ corresponding to consecutive flat segments, and δE_{tik} with $i = 2, 3, \ldots, 7$ ($k = i + 1$) as taken from Figure 7b and calculated according to Equation (45), are listed in Table II.

We note that the total luminescence (F) quenching is due to the quenching of its delayed part (F_{DF}) and therefore the effect can start at a certain level of the

TABLE II

Quantity \ 1	2	3	4	5	6	7
I[10^{13}quanta/cm^{2}s]	2	3.4	8.2	16	22	27.5
δ	0.0055	0.050	0.095	0.152	0.190	0.232
ΔE_{tik}[k_BT]*	2.24	0.63	0.5	0.22	0.19	

* The calculations have been done with $\alpha = 10^4 cm^{-1}$ (λ_{ex} = 436nm; unpolarized) and $\gamma_{TS} = 5 \times 10^{-10} cm^3 s^{-1}$ [27,29].

excitation when the luminescence efficiency becomes an increasing function of the excitation intensity.[27,28] In our case it occurs at $I \gtrsim 10^{13}$ quanta/cm^{2}s (see the insert in Figure 7b). At this excitation level the concentration of trapped holes $n_t = \Delta\beta/K_{Th} \simeq 10^{12}$ cm^{-3} as calculated using Equation (33) with $\delta = 0.1\%$, $K_{Th} = 2 \times 10^{-9}$ cm$^3 s^{-1}$,[32,35] and $k_s \simeq k_{TOT}$.[27] On the other hand, the concentration (N_0) of macrotraps can be smaller than 10^{12} cm^{-3} (for example $N_0 = 4.5 \times 10^{11}$ cm^{-3} has been determined for naphthalene crystals).[5]

If we assumed $N_0 < 10^{12}$ cm^{-3} for our tetracene crystal, the trap-filled-limit due to one-carrier occupied macrotraps, would not be detected in the luminescence quenching experiment; the first flat segment corresponding to two-carrier occupied macrotraps and the first energy gap ΔE_{tik} being the gap between E_{t2} and E_{t3}. $\Delta E_{t23} = 2.24\, k_BT \simeq 0.06$ eV at room temperature could then be identified with the (2–3) gap for macrotraps with $\sigma = 1.0$ (cf. Figure 5). The decreasing progression ΔE_{t23}: ΔE_{t34}: ΔE_{t45}: ΔE_{t56}: $\Delta E_{t67} = 11.8$: 3.3: 2.6: 1.2: 1, with exception of the first term, resembles the progression ΔE_{t23}: ΔE_{t34}: ΔE_{t45}: ΔE_{t56}: $\Delta E_{t67} = 5$: 3: 2.1: 1.4: 1 of the energy spacing relations between the consecutive energy levels with $N = 2, 3, 4, 5, 6, 7$ for the macrotrap with $r_0 = 10^3$ Å and $\sigma = 1.0$ (see Figure 5). The first term disagreement can be caused by an overlap with the level sequence of another macrotrap. An alternate explanation for the observed cascades in δ is that they may be caused by periodic increases in the carrier density trapped sequentially in a shallow macrotrap with large σ.

Approximation II: $\beta > \beta_t$, $5 \times 10^{14} \lesssim I \lesssim 10^{16}$ quanta/cm^{2}s.
The flat segments of δ on the falling part of the curve in Figure 7a correspond now to consecutive trapping levels determined by the position of the quasi-Fermi level given by

$$E_t = E_F = k_BT \ln \frac{\theta N_{\text{eff}}}{n_f - \theta n_t}. \tag{46}$$

The energy spacing between two adjacent (i, $k = i + 1$) trapping levels can now

be expressed as

$$\Delta E_{tik} = k_B T \ln \left(\frac{\theta_1}{\theta_k} \frac{n_{fk} - \theta_k n_{tk}}{n_{fi} - \theta_i n_{ti}} \right). \tag{47}$$

In order to employ Equation (47) for calculations to be compared with the experiment we have to associate n_f, n_t and θ with the voltage applied to the crystal and excitation light intensity. The first step is to calculate β [Equation (36)] and β_t [Equation (41)] which allows us to calculate n_f, n_t and

$$\theta = \frac{n_f}{n_f + n_t}. \tag{48}$$

In contrast to Approximation I, here, β is a function of $[T]$ and the latter can be obtained from simultaneous solution of Equations (32) and (40),

$$[T] \simeq \frac{\beta k_r}{2AR_{\mathrm{Th}}} \left(1 + \frac{4\alpha A R_{\mathrm{Th}}}{k_r} I \right)^{1/2}. \tag{49}$$

Then, according to Equations (36), (40) and (49)

$$\beta = \frac{1}{2} \left[\beta_t + \left(\beta_t^2 + \frac{4AR_{\mathrm{Th}}}{k_r} \alpha I \right)^{1/2} \right], \tag{50}$$

where

$$\beta_t = k_r^{-1} \left(\beta_0^2 k_r^2 + \frac{2A^2 \alpha R_{\mathrm{Th}}^2}{\gamma_{\mathrm{TS}}} I\delta \right)^{1/2}. \tag{51}$$

β_t has been derived using its definition given by Equation (41) and employing Equation (33) with $\beta = \beta_t$.

Thus, having β and β_t determined by the experimental results for δ as a function of I, we can calculate

$$n_t = \frac{\beta_t - \beta_0}{K_{\mathrm{Th}}}, \tag{52}$$

$$n_f = \frac{\beta_t}{R_{\mathrm{Th}}} \left(\frac{\beta}{\beta_t} - 1 \right), \tag{53}$$

and θ, and ΔE_{tik} follow directly from Equations (48) and (47), respectively. The results obtained for the flat segments in the falling part of the experimental $\delta(I)$ plot in Figure 7a are summarized in Table III. Inspection of Table III allows us to conclude that ΔE_{tik} does not obey any monotonic dependence on I and its values fall in the range below $0.5\, k_B T$. Since, following the decreasing progression in ΔE_{tik}

TABLE III*

i	I [ph/cm²s]	β_t [$10^{6}s^{-1}$]	β [$10^{6}s^{-1}$]	n_t [$10^{13}cm^{-3}$]	n_f [$10^{13}cm^{-3}$]	n_f/n_t	$n_{tot}=n_f+n_t$ [$10^{13}cm^{-3}$]	θ	ΔE_{tik} [k_BT]
1	1.7×10^{15}	1.19	1.87	1.98	0.68	0.34	2.66	0.26	0.22
2	2.4×10^{15}	1.35	2.18	2.30	0.82	0.36	3.12	0.26	0.49
3	4.0×10^{15}	1.65	2.74	2.90	1.09	0.38	3.99	0.27	0.37
4	6.7×10^{15}	1.94	3.41	3.48	1.47	0.42	4.95	0.30	0.01
5	9.0×10^{15}	2.07	3.83	3.74	1.76	0.47	5.23	0.32	0.23
6	17.0×10^{15}	2.44	4.99	4.48	2.56	0.57	7.04	0.36	

* The data contained in the Table have been obtained with the following values of the constants appearing in the employed formulae: $R_{Tn} = 10^{-8}cm^3s^{-1}$ (the exact value of this constant is not known; it is therefore assumed that the ratio $R_{Tn}/K_{Tn} = 10$ obeys for tetracene similar to anthracene crystal [36]; $k_r = 4\times10^{6}s^{-1}$ obtained from the relation $k_r = v_r/d_r$, where $d_r = 5Å$ is the recombination distance of a charge carrier and $v_r = 0.2cm/s$ is the recombination velocity of the carrier at the electrode (v_r has been calculated basing on the SCLC-saturation current transition as proposed by Pope and Swenberg [41]); $A = 3\times10^{-5}s^{-1}$ treated as the product of the hole injection efficiency $\eta_+ = 10^{-2}$ and the total quenching rate for the triplet excitons at the pure water contact $k_q = 3\times10^{7}s^{-1}$ as determined by Kalinowski [31]); the remaining constants used as previously quoted.

for $I \ll 10^{15}$ quanta/cm²s (see Approximation I), one would expect further decrease in ΔE_{tik}, that is $\Delta E_{tik} < 0.2\,k_BT$, some of the values for $I \gtrsim 10^{15}$ quanta/cm²s seems to be too high. This can be explained by increasing with I contribution of triplet exciton-free charge carrier interaction (see an about two-fold increase in n_f/n_t) to the measured effect. If we rewrite Equation (47) in a form

$$\Delta E_{tik} \simeq k_BT \ln \left[\frac{\theta_i n_{tk}}{\theta_k n_{ti}} \frac{\left(\frac{n_{fk}}{n_{tk}} - \theta_k\right)}{\left(\frac{n_{fi}}{n_{ti}} - \theta_i\right)} \right], \tag{54}$$

then the free charge carrier contribution is due to the factor with round brackets. It is easily seen that putting it to be equal unity leads to

$$\Delta E_{tik} = k_BT \ln \left(\frac{\theta_i}{\theta_k} \frac{n_{tk}}{n_{ti}} \right) \tag{55}$$

which, as expected gives all values of $\Delta E_{tik} < 0.2\,k_BT$. The lack of monotonic progression in these small values of energy gaps seems to be a natural consequence

of finite resolution of the experimental method and, on the other hand, interference of highly populated levels from different type macrotraps.

4. SUMMARY

We have proposed a model of multi-charge trapping by spatially extended domains (macrotraps) present in molecular organic crystals. By virtue of the quantization of the charge, the macrotraps energy can have only certain discrete values E_{t1}, E_{t2}, E_{t3}, . . . characteristic for a given macrotrap. Calculations of E_{ti} ($i = 1, 2, 3, \ldots n$) are presented, using the approximation of a continuous charge distribution and previously determined typical macrotrap parameters obtained from an analysis of SCLC data on anthracene single crystals. The continuous charge data distribution approach reproduces well the energy levels obtained from the exact calculations with discrete charges located according to the symmetry resulting from the number of charges occupying a macrotrap.

We have also proposed a straight-forward method for interpreting the cascade-like pattern behaviour of various characteristics of the electronic processes on the elaborated multi-charge trapping (MCT) model. The model reproduces the principal experimental results illustrated in details by the charge-induced changes of the triplet exciton lifetime in anthracene and total fluorescence quenching in tetracene crystals. The physical difference between multi-charge trapping and trapping by a set of separate individual traps is emphasized and discussed in terms of the MCT approach. Although the general features of the cascade-like patterns can be explained by either of these two trapping processes, the MCT approach allows to show that the energy spacings corresponding to successive cascade steps (especially at low charge density level) can be an order of magnitude larger than k_BT in contrast to the result from the trapping by separate individual traps differentiated in energy depth (by clustering of successive dimers for example). At high charge density level the energy gaps become comparable and even smaller than k_BT. The experimental ability of detection such small energy spacings also warrants emphasis.

Acknowledgements

We are grateful to Prof. Martin Pope for useful correspondence and for his clarifying comments. This work is partly based on the results of a research project supported by the Polish Academy of Sciences under Program CPBP 01.14.

References

1. J. Kalinowski, Excitonic Interactions in Organic Molecular Crystals, Technical Univ., Gdańsk (1977) (in Polish with English Abstract).
2. E. A. Silinsh, Organic Molecular Crystals (Their Electronic States), Springer Verlag, Berlin (1980).
3. K. C. Kao and G. Hwang, Electrical Transport in Solids, Pergamon Press, London (1981).
4. M. Pope and C. E. Swenberg, Electron Processes in Organic Crystals, Clarendon, Oxford (1982).
5. J. Kalinowski, J. Godlewski and P. Mondalski, *Mol. Cryst. Liq. Cryst.*, **175**, 67 (1989).
6. J. Kalinowski, J. Godlewski and P. Mondalski, The International Conference on the Science and

Technology of *Defect Control in Semiconductors*, Yokohama, 17–22 Sept. 1989. Abstracts Book p. 250. Proceedings, K. Sumino, ed. North Holland, Amsterdam (1990), vol. II, p. 1705.
7. M. Pope and H. Kallmann, *Israel J. Chem.*, **10**, 269 (1972).
8. M. Pope and J. Burgos, unpublished data.
9. G. Aprilisi, T. Garofano, F. Nava and M. Santangelo, *Nuovo Cimento*, **1B**, 85 (1971).
10. J. Levinson, S. Z. Weisz, A. Cobas and A. Rolon, *J. Chem. Phys.*, **52**, 2794 (1970).
11. S. Z. Weisz, J. Levinson and A. Cobas, in *Proc. Third Photoconductivity Conf., Stanford, 12–15 August, 1969*. E. M. Pell, ed., Pergamon, Oxford (1971).
12. V. Ern, H. Bouchriha, J. Fourny and G. Delacote, *Solid State Commun.*, **9**, 1201 (1971).
13. H. Bouchriha, G. Delacote, P. Dellanoy and M. Schott, *Journ. Physique*, **35**, 577 (1974).
14. L. Peter and G. Vaubel, *Phys. Stat. Sol. (b)*, **48**, 587 (1971).
15. J. Kalinowski and J. Godlewski, in Proc. Summer School *Electcrical Properties of Organic Solids, Karpacz, 1–7 Sept., 1974*, Tech. Univ. Wrocław (1974), p. 109.
16. J. Kalinowski and J. Godlewski, *The Second Nat. Conf. on Luminescence, Toruń, 16–19 Sept. 1974*, Abstracts p. 51 (in Polish).
17. O. H. Le Blanc, *J. Chem. Phys.*, **35**, 1275 (1961).
18. J. Kalinowski, J. Godlewski and J. Gliński, *Acta Phys. Polon.* **A65**, 413 (1984).
19. W. Helfrich, in *Physics and Chemistry of the Organic Solid State*, D. Fox, M. M. Labes and A. Weissberger, eds. Wiley, New York (1967), vol. III, p. 1.
20. H. Kokado and W. G. Schneider, *J. Chem. Phys.*, **40**, 2937 (1964).
21. J. M. Thomas, J. O. Williams and G. A. Cox, *Trans. Faraday Soc.*, **64**, 2496 (1968).
22. M. Gamoudi, N. Rosenberg, G. Guillaud, M. Maitrot and G. Mesnard, *J. Phys. C: Solid State Phys.*, **7**, 1149 (1974).
23. A. Samoć, M. Samoć, J. Sworakowski, J. M. Thomas and J. O. Williams, *Phys. Stat. Sol. (a)*, **37**, 271 (1976).
24. C. E. Swenberg and W. I. Stacy, *Chem. Phys. Letters*, **2**, 327 (1968).
25. R. E. Merrifield, P. Avakian and R. P. Groff, *Chem. Phys. Letters*, **3**, 155 (1969).
26. N. Geacintov, M. Pope and F. Vogel, *Phys. Rev. Letters*, **22**, 593 (1969).
27. M. Pope, N. Geacintov and F. Vogel, *Mol. Cryst. Liq. Cryst.*, **6**, 83 (1969).
28. M. Pope, N. E. Geacintov, D. Saperstein and F. Vogel, *J. Lumin.*, **1, 2**, 224 (1970).
29. V. Ern, J. L. Saint-Clair, M. Schott and G. Delacote, *Chem. Phys. Letters*, **10**, 287 (1971).
30. J. Kalinowski, R. Jankowiak and H. Bässler, *J. Lumin.*, **22**, 397 (1981).
31. J. Kalinowski, *J. Lumin.*, **11**, 393 (1976).
32. J. Kalinowski and J. Godlewski, *Chem. Phys.*, **32**, 201 (1978).
33. G. Vaubel and H. Baessler, *Phys. Stat. Sol.* **37**, K31 (1970).
34. P. Delannoy and M. Schott, *Phys. Stat. Sol.*, **70**, 119 (1975).
35. J. Kalinowski and J. Godlewski, *Phys. Stat. Sol. (a)*, **20**, 403 (1973).
36. E. L. Frankevich, I. A. Sokolik and L. V. Lukin, *Phys. Stat. Sol. (b)*, **54**, 61 (1972).